

Carbon, Nitrogen, and Oxygen Galactic Gradients: A Solution to the Carbon Enrichment Problem

Leticia Carigi

*Instituto de Astronomía, Universidad Nacional Autónoma de México, Apdo. Postal 70-264,
México 04510 D.F., Mexico*

carigi@astroscu.unam.mx

Manuel Peimbert

*Instituto de Astronomía, Universidad Nacional Autónoma de México, Apdo. Postal 70-264,
México 04510 D.F., Mexico*

peimbert@astroscu.unam.mx

César Esteban

Instituto de Astrofísica de Canarias, E-38200, La Laguna, Tenerife, Spain

cel@ll.iac.es

and

Jorge García-Rojas

Instituto de Astrofísica de Canarias, E-38200, La Laguna, Tenerife, Spain

jogarcia@ll.iac.es

ABSTRACT

Eleven models of Galactic chemical evolution, differing in the carbon, nitrogen, and oxygen yields adopted, have been computed to reproduce the Galactic O/H values obtained from H II regions. All the models fit the oxygen gradient, but only two models fit also the carbon gradient, those based on carbon yields that increase with metallicity due to stellar winds in massive stars (MS) and decrease with metallicity due to stellar winds in low and intermediate mass stars (LIMS). The successful models also fit the C/O versus O/H evolution history of the solar vicinity obtained from stellar observations. We also compare the present day N/H gradient and the N/O versus O/H and the C/Fe, N/Fe, O/Fe versus

Fe/H evolution histories of the solar vicinity predicted by our two best models with those derived from H II regions and from stellar observations. While our two best models fit the C/H and O/H gradients as well as the C/O versus O/H history, only Model 1 fits well the N/H gradient and the N/O values for metal poor stars but fails to fit the N/H values for metal rich stars. Therefore we conclude that our two best models solve the C enrichment problem, but that further work needs to be done on the N enrichment problem. By adding the C and O production since the Sun was formed predicted by Models 1 and 2 to the observed solar values we find an excellent agreement with the O/H and C/H values of the solar vicinity derived from H II regions O and C recombination lines. Our results are based on an IMF steeper than Salpeter’s, a Salpeter like IMF predicts C/H, N/H, and O/H ratios higher than observed. One of the most important results of this paper is that the fraction of carbon due to MS and LIMS in the interstellar medium is strongly dependent on time and on the galactocentric distance; at present about half of the carbon in the interstellar medium of the solar vicinity has been produced by MS and half by LIMS.

Subject headings: Galaxy: abundances—Galaxy: evolution— H II regions— ISM: abundances—Stars:mass loss

1. Introduction

Many chemical evolution models have been recently made to explain the chemical composition of the solar vicinity (e.g. Henry, Edmunds, & Köppen 2000, Liang, Zhao & Shi 2001, Chiappini, Matteucci & Meynet 2003a, Chiappini, Romano, & Matteucci 2003b, Akerman et al. 2004). In addition a few models have been computed to explain the behavior of C/O as a function of the distance to the Galactic center (e.g. Hou, Prantzos, & Boissier 2000, Carigi 2003, Chiappini et al. 2003b, Gavilán, Buell, & Mollá 2005). In this paper the word gradient of an abundance ratio will be used to denote the galactocentric slope and the absolute value in the solar vicinity.

Most of the Galactic chemical evolution models predict a similar history for C/O versus O/H at the solar vicinity, but make different predictions for the behavior of C/O at different Galactocentric distances. All authors agree that both massive stars (MS) and low and intermediate mass stars (LIMS) play a significant role in the C production of the solar vicinity, nevertheless some authors find that most of the C is due to MS (e.g. Carigi 2000, 2003; Henry et al. 2000) while other authors find that most of the C is due to LIMS (e.g. Chiappini et al. 2003b). The different predictions on: the C/H value in the solar

vicinity, the Galactic C/O gradient, and the relative importance of MS and LIMS in the C production are mainly due to the stellar chemical evolution models obtained with different C yields. To discriminate among the sets of yields we need additional observational constraints to those used before. The C/H and O/H values derived from H II regions at different galactocentric distances by Esteban et al. (2004a, hereinafter Paper I), provide us with the additional constraints necessary to study this problem. In this paper we present eleven different chemical evolution models for the Galaxy, based on combinations of eight different stellar yields, to try to fit the observed C/O gradient.

It is difficult to study the C enrichment of the Galaxy because C is produced by MS and LIMS and the evolution of both types of objects depends on: stellar winds, the convection treatment, and the $^{12}\text{C}(\alpha,\gamma)^{16}\text{O}$ rate, and an exact treatment of these three ingredients of the models is not yet available (e.g. El Eid et al. 2004, Herwig & Austin 2004). Due to these reasons many different estimates of the C yields for MS and LIMS are available in the literature. We have called “the C enrichment problem” the difficulty of estimating the proper C yields for MS and LIMS. In this paper we explore different solutions to the C problem studying only the effect of the stellar winds on the value of C yields.

It is even more difficult to study the N enrichment of the Galaxy for the following reasons: it is produced by LIMS and MS, it can have a primary or secondary origin, and in general its abundance is considerably smaller than that of C and O. This last point implies that an uncertainty in the secondary production of N will affect considerably more the N abundances than the C and O abundances. Consequently on theoretical grounds the predicted O and C values are more robust than the N values. From observations of H II regions the abundances of C and O are of higher quality than those of N for the following reasons: for O we observe all the stages of ionization, for carbon we observe only the C^{++} fraction and an ionization correction factor, ICF, is needed to correct for the unseen ions, fortunately for C the ICF is small. On the other hand for N we observe only the N^+ fraction which in general is not the most abundant ion, and consequently large ICFs are needed to obtain the total N abundance. Moreover the C and O abundances used in this paper are based on recombination lines that are almost independent of the temperature structure of the H II regions, while the N^+ abundances are based on collisionally excited lines that do depend on the temperature structure of the nebulae. To reach agreement between the different N/H observational data as well as between the observations and the predicted N/H values will be called “the nitrogen enrichment problem”.

We will use also the C/Fe, N/Fe, O/Fe versus Fe/H enrichment histories that provide us with additional checks to the models presented in this paper.

2. Observational Constraints

Our models will be compared with unevolved F and G stars and Galactic H II regions. In this work the data used as observational constraints are the following: i) the C/H and O/H abundances from Galactic H II regions presented in Paper I and the N/H abundances presented in Table 1 and Figure 1 (Esteban et al. 2004b, García-Rojas et al. 2004, and in preparation), ii) the H, C, N, O, and Fe abundances from main sequence stars in the solar vicinity obtained by Santos, Israelian, & Mayor (2000), Takeda et al. (2001), González et al. (2001), Sadakane et al. (2002), Akerman et al. (2004), and Israelian et al. (2004), and iii) the H, C, N, O, and Fe solar abundances (Asplund, Grevesse, & Sauval 2005).

In Paper I new C/H and O/H gaseous values for eight H II regions between 6 and 11 kpc are presented, adopting a Galactocentric distance for the Sun of 8 kpc (see Fig. 2 of Paper I). These C/H and O/H values have been increased by 0.10 dex and 0.08 dex, respectively, due to the fraction of C and O embedded in dust grains (Esteban et al. 1998). Based on these data the C/H, O/H and C/O slopes of the gradients are -0.103 , -0.044 , and -0.058 dex kpc^{-1} , respectively.

The values of Table 1 were obtained from the Very Large Telescope and the Ultraviolet Echelle Spectrograph (Esteban et al. 2004, García-Rojas et al. 2004, and in preparation). The N^+ abundances were obtained from collisionally excited lines taking into account the temperature structure by adopting t^2 values different from 0.00 (see Peimbert 1967 for the definition of t^2), the increase in the N/H values due to this effect amounts to about 0.21 dex. The total nitrogen abundances were obtained based on the ICF values derived from the models by Mathis & Rosa (1991), note that these ICF values yield N abundances about 0.11 dex higher than those derived from the usual formulation by Peimbert and Costero (1969) where it is assumed that N^+/O^+ is equal to N/O .

In Figure 1 we present the N/H, N/O, and N/C values versus Galactocentric distance based on the N/H values presented in Table 1 and the C/H and O/H values presented in Paper I. The linear fits to the data, giving equal weight to each value, are:

$$12 + \log(\text{N}/\text{H}) = (8.517 \pm 0.156) - (0.085 \pm 0.020)R_G,$$

$$\log(\text{N}/\text{O}) = (-0.606 \pm 0.113) - (0.042 \pm 0.015)R_G,$$

$$\log(\text{N}/\text{C}) = (-0.979 \pm 0.190) + (0.017 \pm 0.024)R_G.$$

It is not possible to estimate the total Fe abundances based on the Fe gaseous abundances derived from H II regions data because most of the Fe atoms are embedded in dust grains (Esteban et al. 1998). Therefore we will use only the Fe values from stars of the solar vicinity to compare with our models.

Akerman et al. (2004) present C/H, O/H, and Fe/H stellar values from 34 F and G dwarf stars of the Galactic halo and combine their values with similar data from 19 disk stars. Based on these data the C/O value in the solar vicinity drops from $12+\log(\text{O}/\text{H}) \sim 6$ to ~ 7.7 and then increases from $12+\log(\text{O}/\text{H}) \sim 7.7$ to 8.8.

Israelian et al. (2004) present N/H, O/H, and Fe/H stellar values from 31 metal-poor stars and 15 metal rich stars. Based on these data it is found that the N/O values in the solar vicinity increase with O/H with the exception of the N-rich star G64-12. We did not consider those metal-poor stars with only an upper limit in N/H. Santos et al. (2000), Takeda et al. (2001), González et al. (2001), and Sadakane et al. (2002) present C/H stellar values for the metal rich stars by Israelian et al..

3. Chemical Evolution Models

All models are built to reproduce the observed gas fraction distribution of the Galaxy and the observed O/H H II region values from 6 to 11 kpc at 13 Gyr, the age of the model, the time elapsed since the beginning of the formation of the Galaxy. The observed O/H values might be extrapolated to the 4 to 16 kpc range. The models do not reach the central regions of the Galaxy because the evolution of the central regions might not correspond to an extrapolation of the disk values to the center for the following reasons: a) the bulge has a different chemical evolution history; b) the effect of the bar has to be considered; c) the extrapolation of the models to higher metallicities might not be correct due to saturation effects.

The chemical evolution models for the solar vicinity of Akerman et al. (2004) have been extended to follow the chemical history of the Galactic disk in the 4 kpc to 16 kpc range, under the following assumptions:

i) The total surface mass density adopted as a function of time and Galactocentric distance r is given by

$$\frac{d\sigma_{\text{gas+stars}}}{dt} = A(r)e^{-t/\tau_{\text{halo}}} + B(r)e^{-(t-1\text{Gyr})/\tau_{\text{disk}}}, \quad (1)$$

where the formation timescales $\tau_{\text{halo}} = 0.5$ Gyr and $\tau_{\text{disk}} = 6 + (r/r_{\odot} - 1)8$ Gyr, and the constants $A(r)$ and $B(r)$ are chosen to match the present-day radial distribution of gas surface mass density (Prantzos 2003); the total surface mass density is given by $(\sigma_{\text{tot}}(r_{\odot}, t_g) = 50e^{-(r-8\text{kpc})/3.5\text{kpc}} M_{\odot}pc^{-2})$, where we have adopted the halo to disk mass ratio of the solar vicinity for all Galactocentric distances.

ii) The star formation rate is proportional to a power of σ_{gas} and σ_{tot} : $SFR(r, t) =$

$\nu \sigma_{gas}^{1.4}(r, t) \sigma_{tot}^{0.4}(r, t)$, where ν is a constant in time and space. In order to improve the agreement of the halo to disk abrupt change in C/O at $12+\log(O/H) \sim 8$, we assume a ν value five times higher during the halo formation than that adopted for the disk.

A ν value for the disk of 0.016 has been adopted for all models, with the exception of those models that assume the yields by Woosley & Weaver (1995). For these yields the adopted ν value is 0.019.

iii) The Initial Mass Function (IMF) adopted is the one proposed by Kroupa, Tout & Gilmore (1993, KTG) in the mass interval given by $0.01 < m/M_{\odot} < 80$. The KTG IMF is a three power-law approximation, given by $IMF \propto m^{-\alpha}$ with $\alpha = -1.3$ for $0.01 - 0.5 M_{\odot}$, $\alpha = -2.2$ for $0.5 - 1.0 M_{\odot}$, and $\alpha = -2.7$ for $0.5 - 80 M_{\odot}$.

iv) In order to study the contribution to the C, N, and O enrichment of the interstellar medium, ISM, due to stellar evolution we have assumed different sets of stellar yields, all dependent on metallicity.

For massive stars (MS), those with $8 < m/M_{\odot} < 80$, we have used the following five sets of yields: a) Chieffi & Limongi (2002) for initial metallicities (by mass) $Z = 0.0$; b) Meynet & Maeder (2002, MM02) for $Z = 10^{-5}$, $Z = 0.004$, and $Z = 0.02$; c) For all elements MM02 for $Z = 1 \times 10^{-5}$ and $Z = 0.004$, for C and O Maeder (1992, M92) for $Z = 0.02$ (high mass-loss rate) for N MM02 for $Z = 0.02$; d) Woosley & Weaver (1995, WW95) from $Z = 10^{-4}$ to $Z = 0.02$; e) Portinari, Chiosi, & Bressan (1998, PCB98) from $Z = 0.0004$ to $Z = 0.05$.

For low and intermediate mass stars (LIMS), those with $0.8 \leq m/M_{\odot} \leq 8$, we have used the following three sets of yields: a) Meynet & Maeder (2002, MM02) for $Z = 1 \times 10^{-5}$; b) van den Hoek & Groenewegen (1997, vdHG) from $Z = 0.001$ to $Z = 0.04$ with constant or variable η (parameter that represents the importance of mass loss during the AGB phase) as a function of Z , where in the first case $\eta = 4$ for all Z and in the second case $\eta = 1$ for $Z = 0.001$, $\eta = 2$ for $Z = 0.004$, and $\eta = 4$ for all other Z values; and c) Marigo, Bressan, & Chiosi (1996, 1998), and Portinari et al. (1998) from $Z = 0.004$ to $Z = 0.02$, these sets of yields have been labelled MBCP.

For massive stars we have used Fe yields by Woosley & Weaver (1995) (Models B, for 12 to 30 M_{\odot} ; Models C, for 35 to 40 M_{\odot}). For $m > 40 M_{\odot}$, we have extrapolated the Fe yields for $m = 40 M_{\odot}$.

We have assumed that 5 % of the stars with initial masses between 3 and 16 M_{\odot} are binary systems which explode as Type Ia SNe with the yields computed by Thielemann, Nomoto & Hashimoto (1993). This fraction is needed to explain the metallicity distribution

of local G and K dwarf stars.

For each set of yields, linear interpolations for different stellar masses and metallicities were made. For metallicities higher or lower than those available we adopted the yields predicted by the highest or lowest Z available, respectively.

The models fit many observational constraints related to the chemical abundances, for example: the total surface density, the infall rate, and the star formation rate of the solar vicinity and the Galactic disk.

4. Results

4.1. Carbon and oxygen

The essence of this work is to explore the behavior of the C/O gradient in the Milky Way and the C/O history of the solar vicinity. It is important to note that the O/H values depend on the O yields, the initial mass function, and the Galaxy formation history and are well adjusted by all models. While the C/O ratio depends mainly on the C yields, therefore permitting us to discriminate among the C yields available.

In Table 2, we present the following predictions of the models for the present time: i) the C/O value at $r = r_{\odot}$, and ii) the C/O value of the slope of the gradient for the 6 to 11 kpc range, zone that corresponds to the observations of Paper I. From this table, it can be noted that:

i) The C/O value at the solar Galactocentric radius is reproduced by Models 1, 2, 9, and 10 that adopt two kinds of stellar yields. In Models 1, 2, and 9 we adopted the C and O yields for MS with high stellar winds (M92, PCB98) and the C yields for LIMS that decrease with Z (MBCP or vdHG.var). In Model 10 we adopted the C and O yields for MS without stellar winds (WW95) and the C yields for LIMS that decrease with Z (vdHG.var).

ii) Models 3 to 8 and 11 predict for $r = r_{\odot}$ C/O values 0.1 to 0.4 dex lower than observed.

iii) The C/O gradient is only reproduced by Models 1 to 4 that assume for massive stars the C MM02 yields for $10^{-5} \leq Z \leq 0.004$ and the C M92 yields for $Z = 0.02$.

iv) Models 5 to 11 predict C/O gradients flatter than observed. For Models 5 to 8 the MS MM02 yields with $Z = 0.02$ have winds with lower mass loss rates than those by M92, producing a smaller amount of C. For Model 9 the C/O gradient is almost flat because the MS PCB98 yields with $Z > 0.02$ include intense winds, which occur before these stars synthesize

C; therefore, their C yields become similar to those without stellar winds (Carigi, 2000). For Models 10 and 11 the MS WW95 yields do not include stellar winds and consequently the C yields do not depend on Z .

v) The low C/O values predicted by Models 4 and 8 are mainly due to the MM02 yields for LIMS, the lowest ones considered in this paper, because the MM02 yields did not extend to the thermal-pulse AGB phase, consequently the third dredge-up and the hot-bottom burning stages were not included. Moreover, the computations based on the MM02 yields for LIMS are somewhat uncertain because the only yields available are from $2 M_{\odot}$ to $7 M_{\odot}$ for $Z = 10^{-5}$, and for $3 M_{\odot}$ in for $Z = 0.004$ and $Z = 0.02$.

vi) Models 2 and 6, with vdHG.const yields, predict higher C/O values than Models 3 and 7, with vdHG.var yields, because the vdHG.const yields are computed with $\eta = 4$ while vdHG.var yields are computed with η between 1 and 4. With higher η values the stars lose more gas and the AGB lifetimes become shorter, reducing the C yields.

vii) The highest C/O values with the same MS yields were predicted by Models 1 and 5, because the yields by MBCP for LIMS were computed with η values lower than those assumed by vdHG.

As mentioned in the Introduction the C enrichment is complex and depends on many variables. Therefore, we decided to evaluate the relative importance of MS and LIMS in the production of C and to compute the fraction of C in the ISM due to both types of stars. In Table 3, we present the C processed and ejected to the ISM by MS, LIMS and Type Ia SNe during the whole evolution of the solar vicinity. From this table it can be noted that: a) Models 1 and 2, that are the two models that best fit the data, predict that MS produce between 48 % and 50 % and LIMS produce between 50 % and 47 % of the ISM present-day carbon abundance, b) the unsuccessful models predict that the C produced by MS varies from 36 % to 75 % and the C produced by LIMS varies from 62 % to 26 %, c) the rest of the C is produced by type Ia SNe. The relative importance of the C production of MS and LIMS changes with time (Akerman et al. 2004) and with Galactocentric radius.

In Figure 2 we present the cumulative C enrichment of the ISM of the solar vicinity as a function of time and O/H for Models 1 and 2. As can be seen from the figure MS dominate the C enrichment at early times, $12 + \log(\text{O}/\text{H}) < 8$. For latter times, $12 + \log(\text{O}/\text{H}) > 8$, the contributions by MS and LIMS become comparable. At $12 + \log(\text{O}/\text{H}) \sim 8$ the contribution of LIMS to the C enrichment increases because the LIMS formed in the halo end their evolution ejecting freshly made C, note that the low Z LIMS eject more C than the high Z ones. For $12 + \log(\text{O}/\text{H}) > 8.5$ the relative decrease in C production by LIMS is due to the higher contribution of the high Z MS to the C production, and the lower contribution

of the high Z LIMS.

In Table 4 we present the fraction of C due to MS and LIMS in the ISM for Models 1 and 2 at different Galactocentric distances. As expected, the fraction of C present in the ISM produced by MS increases with decreasing r (for higher O/H values), because for MS the C yields increase with Z , while for LIMS they decrease with Z .

To make a detailed comparison with the observed abundances we present in Table 5 the C/H and O/H predicted values by Models 1 and 2 for the ISM at the time the Sun was formed (4.57 Gyr ago) and at the present time.

In the left panel of Figure 3 we show the C/O versus O/H enrichment history for the solar vicinity predicted by Models 1 and 2. Also in this figure we present three types of observations: a) stellar values that are well fitted by Models 1 and 2 with the exception of those objects $C/O < -0.8$ dex, b) values for the two closest H II regions in Galactocentric distance to the solar vicinity, Orion and NGC 3576, that are perfectly fitted by Model 1 and 2, c) the solar values that are also perfectly fitted by Models 1 and 2.

In the right panels of Figure 3 we show the fit of Models 1 and 2 to the data presented in Paper I. All the models were constructed to reproduce the O/H values derived from H II regions, but Models 1 and 2 also produce an excellent fit to the C/H H II region values and a good fit to the C/O gradient, while the other models do not. Note that for Galactocentric distances smaller than 6 kpc the C/O values predicted by the models start to saturate. Additional observational data as well as a model that includes the behavior of the bulge are needed to study the regions with $r < 4$ kpc. For Galactocentric distances, larger than 11 kpc, the C/O ratio predicted by Models 1 and 2 flattens and again additional observations are needed to test the models. The fit to the observations corresponds to the $6 < r(\text{kpc}) < 11$ range, therefore Models 1 and 2 need to be tested for $r < 6$ kpc and $r > 11$ kpc based on future observations.

4.2. Nitrogen

To constrain further the models of chemical evolution of the Galaxy and to try to discriminate between Models 1 and 2 we decided to study the enrichment of nitrogen during the history of the Galaxy.

In Models 1 and 2, for $Z = Z_{\odot}$, we have assumed N yields from MM02, computed with rotation and stellar winds; while for C and O we have used yields from M92, computed with stellar winds with a higher mass loss rate than those by MM02. The effects of stellar winds

are very important for the C and O yields, but not for the N yields; while the effects due to rotation are more important for the N yields than for the C and O yields.

In Figure 4 we present the cumulative N enrichment of the ISM of the solar vicinity as a function of time and O/H for Models 1 and 2. As can be seen from the figure MS dominate the N enrichment at very early times, $12 + \log(\text{O}/\text{H}) < 6.5$. For latter times, $12 + \log(\text{O}/\text{H}) > 6.5$, the contributions LIMS become more important. The percentage of N by MS increases with $12 + \log(\text{O}/\text{H})$ higher than 8.1 due to the increasing importance of secondary production in MS with increasing O/H.

In Table 6 we present the fraction of N due to MS and LIMS in the ISM for Models 1 and 2 at different Galactocentric distances. As expected, the fraction of N present in the ISM produced by MS increases with decreasing r (for higher O/H values), but in the computed range never produce a higher fraction of N than LIMS. The main reason for this increased production of N by MS is that most of the N is produced by a secondary process.

In the left panel of Figure 5 we present the N/O versus O/H enrichment history for the solar vicinity predicted by Models 1 and 2. Also in this figure we present four types of observations: a) values for metal poor stars that are well fitted by Model 1 with the exception of G6412 that appears to be nitrogen rich, b) values for the two closest H II regions in Galactocentric distance to the solar vicinity, Orion and NGC 3576, that are perfectly fitted by Model 1, c) the solar values that are intermediate between Models 1 and 2, and that show an N/O excess relative to H II regions of about 0.1 dex, and d) values for metal rich stars that appear to be better adjusted by Model 2, but that on average are about 0.3 dex higher than the N/O values determined from Orion and NGC 3576. Also in Table 5 we present the N/H values for ISM predicted by Models 1 and 2 at the time the Sun was formed and at the present time.

In the right panels of Figure 5 we show the present behavior of N/H and N/O for the disk of the Galaxy predicted by Models 1 and 2. In both cases the N/H and N/O H II region values are in excellent agreement with Model 1 and in average about 0.2 dex smaller than those predicted by Model 2.

In the left panel of Figure 6 we present the N/C versus O/H enrichment history for the solar vicinity predicted by Models 1 and 2. Also in this figure we present four types of observations: a) there are only four metal poor stars in common between the data by Akerman et al. (2004), that present C/H and O/H values, and that by Israelian et al. (2004), that present N/H and O/H values, in Figure 6 out of the four stars we present only two of them: HD 140283 and HD 194598, we have an N/C value and two O/H values for each and therefore are plotted twice, the other two stars are not plotted because one of them

only has an upper limit for the N/H value and the other is N rich and falls outside the figure, the observations fall between Models 1 and 2 but are closer to Model 2, b) values for Orion and NGC 3576 that are perfectly fitted by Model 1, c) the solar values that are intermediate between Models 1 and 2, and that show an N/C excess relative to H II regions of about 0.2 dex, and d) values for metal rich stars that appear to be better adjusted by Model 2, but that show N/C values from 0.1 to 0.6 dex higher than the N/C values determined for Orion and NGC 3576.

In the right panels of Figure 6 we show the present behavior of N/C for the disk of the Galaxy predicted by Models 1 and 2. The H II region values are in excellent agreement with Model 1 and are about 0.4 dex smaller than those predicted by Model 2.

4.3. Iron

The history of Fe is different to that of O because in addition to its production by SN of Type II, there is an important contribution due to supernovae of Type Ia. Therefore Fe provides us not only with a consistency check on the models but also with a direct constraint on the production of Type Ia SNe and the Fe yields by massive stars. Moreover C/Fe and N/Fe have been determined in many objects and depend on different physical parameters therefore providing us with additional information. In Table 4 we present the Fe/H values for ISM predicted by Models 1 and 2 at the time the Sun was formed and at the present time.

In Figure 7 we present the C/Fe, N/Fe, and O/Fe observed data for dwarf unevolved stars of the solar vicinity. The axis have been normalized to the solar abundances by Asplund et al. (2005). In the three panels of Figure 7 it is seen that metal rich stars, those in the -0.4 to $+0.4$ [Fe/H] range, the C/Fe, N/Fe and O/Fe ratios fall above the solar value.

Also in Figure 7 we present the C/Fe, N/Fe, and O/Fe versus Fe/H enrichment history for the solar vicinity predicted by Models 1 and 2. The C/Fe and O/Fe versus Fe/H histories for both models are practically the same and fit the solar values reasonably well; for those stars with Fe/H higher than -0.6 dex we find that their C/Fe and O/Fe values are about 0.3 dex above the predictions by the model.

As can be seen in Figure 7 Model 1 predicts a N/Fe ratio about 0.15 dex smaller than the solar value, while Model 2 predicts a N/Fe ratio about 0.2 dex higher than the solar value. Most of the other N/Fe star values presented in Figure 7 lie between both models.

5. Discussion

5.1. Observational constraints

The O/H observations from H II regions that have been used to fit the models are those of Paper I that are based on recombination lines that to a very good approximation are independent of the temperature structure of the nebulae. There are other determinations that are popular, and produce different results, that are based on observations of collisionally excited lines and that do depend strongly on the temperature structure of the nebulae, we will mention three of them, those by Shaver et al. (1983), Deharveng et al. (2000), and Pilyugin, Ferrini, & Shkvarun (2003).

The $12 + \log \text{O/H} = 8.71$ value for the solar vicinity by Shaver et al. (1983) is similar to 8.77, our value; on the other hand they obtain a gradient for the O/H ratio of $-0.07 \text{ dex kpc}^{-1}$ for a solar Galactocentric distance of 10 kpc. For a solar Galactocentric distance of 8.0 kpc, the one adopted by us, their gradient becomes $-0.086 \text{ dex kpc}^{-1}$, considerably steeper than $-0.044 \text{ dex kpc}^{-1}$, our value. Our gradient implies lower O/H values for the inner regions of our galaxy which is consistent with recent suggestions that indicate that the O abundances of H II regions in the inner zones of external spiral galaxies are lower than previously thought (Bresolin, Garnett, & Kennicutt 2004).

The slope of the O/H gradient presented in Paper I is in excellent agreement with that by Deharveng et al. (2000) that amounts to $-0.0395 \pm 0.0049 \text{ dex kpc}^{-1}$, but our O/H ratio for the ISM of the solar vicinity amounts to $12 + \log \text{O/H} = 8.77$, a value 0.29 dex higher than the 8.48 value derived by them. The lower O/H value by Deharveng et al. is due to their adoption of $t^2 = 0.00$ that reduces the O/H value by 0.21 dex relative to the recombination line abundances and to the fraction of O trapped by dust grains that produces a further reduction of 0.08 dex. The similar slope between both groups is probably due to the similar t^2 values for Galactic H II regions at different galactocentric distances that amount to about 0.035 (see Paper I and Table 2).

A similar situation to that by Deharveng et al. (2000) prevails with the O/H gradient by Pilyugin et al. (2003) that present a compilation of 71 observations of 13 galactic H II regions by many authors and derive a slope for the gradient of $-0.048 \text{ dex kpc}^{-1}$ and a $12 + \log \text{O/H} = 8.50$ value for the solar vicinity. The slope of the gradient is in good agreement with that by Deharveng et al. and that presented in Paper I. But their O/H value is 0.27 dex smaller than that obtained by us, again due to their adoption of $t^2 = 0.00$ and the fraction of O trapped by dust grains not included by them.

The N/H H II region values used by us are typically 0.3 dex higher than those used by

other authors. The differences with most authors are due to the adoption by us of $t^2 \neq 0.0$ that yield on average an increase of about 0.2 dex in the N/H values relative to those derived under the assumption that $t^2 = 0.00$; an additional increase of about 0.1 dex comes from the adoption of the ICFs by Mathis & Rosa (1991) that in general are about 0.1 dex higher than those derived under the assumption that $N^+/O^+ = N/O$. Even higher N/H values for the H II regions are needed to reach agreement with the stellar values. We consider unlikely that a systematic difference in the adopted t^2 and ICF values are responsible for the discrepancies between H II regions and stellar values.

The discussion of the N enrichment based on observations alone has an initial problem that has not been solved, namely that H II regions yield N/O and N/C values that in general are considerably smaller than those of metal rich unevolved dwarfs of the solar vicinity; the average difference amounts to 0.2 dex for N/O and to 0.3 dex for N/C. Furthermore the dispersions among the stellar data amounts to 0.6 dex for N/O and 0.5 dex for N/C while for the H II regions the dispersions amount to 0.2 dex in N/O and 0.3 dex in N/C (see Figures 5 and 6). Part of the dispersion of the N/O values from H II regions is due to the presence of an N/O gradient, on the other hand most of the dispersion in the N/O and N/C stellar data is not expected to be due to the dispersion of the ISM abundances at the time these stars were formed because the spreads in age and Galactocentric distances are relative small. The N/O and N/C differences between the metal rich stars and the H II regions need to be sorted out before an agreement between the chemical enrichment history of the Galaxy and the observations can be claimed.

A possible solution to the N differences between metal rich stars and H II regions could be due to a conversion of a small fraction of C into N after the stars were formed. This effect, if present, would help to explain not only the large observational dispersion observed but also the larger N/H values in these stars than in H II regions. The fraction of C transformed into N needs to be small enough to avoid a substantial decrease in the C/H ratio, since this ratio is well explained by the Galactic chemical evolution models.

There are two different sets of solar abundances: a) the one by Asplund et al. (2005), based on a hydrodynamical 3D photospheric model, given by: H = 12.00 dex, C = 8.39 dex, N = 7.78 dex, O = 8.66 dex, and Fe = 7.45 dex, and b) the one by Grevesse & Sauval (1998), based on the classical 1D photospheric model, given by: H = 12.00 dex, C = 8.52 dex, N = 7.92 dex, O = 8.83 dex, and Fe = 7.50 dex. The standard solar models by Bahcall et al. (2004) are in good agreement with the helioseismologically determined sound speed and density as a function of solar radius, the depth of the convective zone, and the surface helium abundance, as long as the models use the Grevesse & Sauval solar abundances. The reasons why the solar abundances by Grevesse & Sauval produce a better fit than those by

Asplund et al. to the standard solar model have to be found. To compare with our Galactic chemical evolution models we have used the Asplund et al. abundances.

The observational constraints from stellar data are not homogeneous. The abundances for all stars but the Sun were determined assuming 1D photospheric models. Moreover some abundances have been computed adopting LTE models and others adopting non-LTE models: a) the O/H values from Akerman et al. (2004) were obtained in non LTE, and the C/O values in LTE; b) the O/H and N/H values from Israelian et al. (2004) were obtained in LTE; and c) the solar abundances from Asplund et al. (2005) were obtained in non-LTE.

The Akerman et al. (2004) values show typical non LTE corrections of -0.1 to -0.2 dex for O/H, but they cannot estimate those corrections for the C/O values. Contrary to the opinion of Akerman et al., Israelian et al. (2004) argue that the O/H and C/H values are almost independent of the non-LTE effects. For metal poor stars the O/Fe values from Israelian et al. are higher than those from Akerman et al.; the differences increase when Fe/H decreases and reach values of about 0.4 dex (see Figure 7).

From the solar experience it is expected that 3D models of metal rich stars will lower the O/H, C/H and N/H values but probably not the N/C and N/O ratios. If the N/C and N/O ratios are not revised downward we have to conclude that N has been enriched in these stars relative to the H II region values.

A better comparison of the stellar abundances with models of Galactic chemical evolution require better analyses of the observational data, it is beyond the scope of this paper to try to homogenize the available observational data.

5.2. Comparison between models and observations

The models were built to reproduce the O/H gradient and the present O/H value of the ISM presented in Paper I. Models 1 and 2 predict for the time the Sun was formed a value of $12 + \log \text{O/H} = 8.66$ for the ISM of the solar vicinity; in excellent agreement with 8.66 ± 0.05 the Asplund et al. (2005) value. Since the Sun was formed the increase in the O/H value of the ISM predicted by Models 1 and 2 amounts to 0.13 dex, in excellent agreement with the observations (see Table 5).

Of the 11 computed models only Models 1 and 2 are able to reproduce: the C/H gradient, the present C/H value in the solar vicinity, and the C/H solar value by Asplund et al. (2005). The other 9 models do not agree with the C observations. The $12 + \log(\text{C/H})$ predicted values by Models 1 and 2 for the solar vicinity at the time the Sun was formed

amount to 8.38 and 8.36, while those for $\log(\text{C}/\text{O})$ amount to -0.28 and -0.30 in very good agreement with the Asplund et al. values that amount to 8.39 ± 0.05 and -0.27 ± 0.05 , respectively (see Table 5). The predicted values for $12 + \log(\text{C}/\text{H})$ at present for the ISM amount to 8.67 and 8.62 for Models 1 and 2, in very good agreement with 8.67 ± 0.07 , the observed value. The predicted values by Models 1 and 2, for $\log(\text{C}/\text{O})$ are -0.12 and -0.17 , while the present value derived in Paper I amounts to -0.10 ± 0.08 .

The predicted C/O versus O/H enrichment history for the solar vicinity of Models 1 and 2 is in reasonable agreement with metal poor unevolved dwarfs, the Solar values, and the values of metal rich stars of the solar vicinity (see Figure 3). The behavior of Model 1 for the halo is similar to that by Akerman et al. (2004). The increase of C/O with O/H is due to two factors: i) the bulk of metal poor LIMS eject large amounts of C in the $7.9 < 12 + \log(\text{O}/\text{H}) < 8.2$ range, and ii) metal rich massive stars eject more C than O for $12 + \log(\text{O}/\text{H}) > 8.2$.

Akerman et al. (2004) were the first to present observational evidence that $\log(\text{C}/\text{O}) \sim -0.6$ for the very metal poorest stars with $12 + \log(\text{O}/\text{H}) \sim 6$; and that for stars in the $6 < 12 + \log(\text{O}/\text{H}) < 7.6$ range the $\log(\text{C}/\text{O})$ value diminished monotonically to -0.95 . The model by Akerman et al. is able to explain the decrease of C/O from -0.6 dex to -0.75 dex because they have assumed the yields by Chieffi & Limongi (2002) for $Z = 0$. Among Pop III yields, those by Chieffi & Limongi present the highest C/O yields ratios. Then the predicted C/O values decrease because the C/O yields ratios by MM02 for $Z = 10^{-5}$, $Z = 0.001$, and $Z = 0.004$ are lower than those for Pop III. As mentioned in Akerman et al. (2004) the minimum C/O value given by the halo objects has not been fitted by previous models nor by the models presented in this paper.

There has been a discussion in the literature on the relative importance of MS and LIMS in the C production by different authors. While Henry, Edmunds, & Köppen (2000) find that MS produce most of the C in the solar vicinity, we find that MS and LIMS produce roughly the same fraction. Our results are different because: a) Henry et al. adopted the C M92 yields for MS increased by factors in the 1.7 to 1.9 range, while we used the yields as presented by MM02 and M92, and b) Henry et al. adopted the Salpeter IMF that predicts a higher number of MS than the KTG IMF adopted by us.

Other authors have discussed the contribution of MS and LIMS to the C enrichment, but their results are not directly comparable to ours. Carigi (2000) only gave a qualitative description of the problem while in this paper we present precise percentages. Carigi (2003) based on the M92 yields presented the instantaneously ejected C as a function of time, including the net C produced by the stars and the amount of initial C that was not converted into heavier atoms; Akerman et al. (2004) based on the MM02 yields presented only the synthesized and instantaneously ejected C as a function of time; while we present only the

cumulative synthesized C up to a given time.

Gavilán et. al (2005) present new models of the C and O chemical evolution of the solar vicinity and the Galactic disk, their models are similar to our models 10 and 11 that predict a flat C/O vs r behaviour. As discussed in Sec 4.1 the flatness is mainly due to the adoption of WW yields for MS. Our best models (1 and 2) do predict a C/O gradient similar to the observed one.

Based on the observed N/H, N/O, and N/C abundances we find that: Model 1 is in agreement with the H II regions and the metal poor stars, Model 2 is in better agreement with the metal rich stars than Model 1, Model 2 does not fit the H II regions and the metal-poor stars, and the solar values are intermediate between Models 1 and 2 (see Table 5 and Figure 5).

With the combined contribution of Type Ia and Type II SNe Models 1 and 2 predict Fe/H values of 7.46 dex and 7.49 dex for the ISM in the solar vicinity at the time the Sun was formed, in excellent agreement with the Asplund et al. (2005) solar value. The present Fe/H values predicted by Models 1 and 2 are 7.72 dex and 7.75 dex, respectively.

The C/Fe and O/Fe solar values are well fitted by Models 1 and 2 (see Figure 7). Alternatively the other stars have on average values about 0.3 dex higher than those predicted by Models 1 and 2. Probably part of the discrepancy is due to difference in the assumptions made in the solar determination by Asplund et al. (2005) and those assumptions made in the determinations for other stars.

It is possible to lower the Fe production predicted by Models 1 and 2, without affecting the C/O versus O/H history, either by the reducing the fraction of the stars that produce Type Ia SNe or by adopting the Fe B yields by WW95 for Type II SNe. In this case the models will produce a better fit to the C/Fe and O/Fe versus Fe/H diagrams for the stars of the solar vicinity, but the predicted solar C/Fe and O/Fe values would become higher than the observed ones. That is, either the Sun is C/Fe and O/Fe poor relative to the other stars, or the C/Fe and O/Fe abundances determinations for the solar vicinity stars present systematic effects relative to the solar determinations by Asplund et al. (2005).

Some of our results might apply to other galaxies. Nevertheless, we like to point out that the star formation history for other galaxies might be different to that of the Galaxy and that tailor made models for representative galaxies are needed to see if our results can be generalized to other objects.

5.3. The use of a Salpeter like IMF

The results presented previously depend on the IMF adopted. Therefore to study the effect of a different IMF we decided to run chemical evolution models with a modified IMF for $m > 1M_{\odot}$.

For $m > 1M_{\odot}$ the KTG IMF shows a very similar slope than that presented by Scalo (1986, with $\alpha = -2.63$) and a steeper slope than that presented by Salpeter (1955, with $\alpha = -2.35$). We will adopt a “Salpeter like” IMF defined as follows: a slope $\alpha = -2.35$ for $m > 1M_{\odot}$ only and the KTG slopes for $m < 1M_{\odot}$.

Since oxygen is produced primarily by massive stars, the computed oxygen abundances are very sensitive to the behaviour of the IMF in the high mass end. A model with a Salpeter like IMF and a mass upper limit (m_{up}) of $80 M_{\odot}$ predicts $12 + \log(C/H) = 8.86$ and $12 + \log(O/H) = 8.95$ for the solar values while for the present time ISM the predicted values are 9.13 and 9.08, respectively; these values are considerably higher than observed. Moreover the predicted gas mass ($18 M_{\odot}pc^{-2}$) is higher than the observed one ($13 \pm 3 M_{\odot}pc^{-2}$). In order to improve the match, we computed several models reducing the upper limit masses of the IMF down to $40 M_{\odot}$. The resulting values for $m_{up} = 40 M_{\odot}$ are $12 + \log(C/H) = 8.54$ and $12 + \log(O/H) = 8.76$ for solar values and 8.81 and 8.94 for the present time ISM values, these values are still considerably higher than the observed ones. Moreover the predicted gas mass ($17 M_{\odot}pc^{-2}$) is still higher than the observed one.

Similarly all models based on a Salpeter like IMF with reasonable m_{up} values ($m_{up} > 40 M_{\odot}$) fail also to reproduce the behavior of the C/O vs O/H enrichment history and the observed gradients simultaneously.

For $m_{up} = 40 M_{\odot}$ the predicted and observed slopes of the C/H gradients are similar, but the predicted slope of the O/H gradient is steeper, and the predicted slope of the C/O gradient is flatter than the observed ones.

The results of this section imply that the observational constraints are strong enough to permit to discriminate among different IMFs. In a future paper we plan to use different IMFs to study exhaustively their effects on the chemical evolution of the solar vicinity and the Galactic disk.

6. Conclusions

We present a set of 11 models built to reproduce the observed O/H gradient including the present solar vicinity O/H value of the ISM. We tested these models with other observational

constraints and the main results are presented below.

Models 1 and 2 predict C/Fe and O/Fe versus Fe/H values from 0 to 0.4 dex smaller than observed. On the other hand, they produce a very good fit to the C/Fe, O/Fe solar values. For the N/Fe versus Fe/H enrichment history Models 1 and 2 differ considerably and the stellar data fall in between. Model 2 is closer to the solar value than Model 1.

There is an observational discrepancy between the N/C and N/O values derived from H II regions and those derived from metal-rich stars of the solar vicinity that has to be sorted out before definitive conclusions of the Galactic N enrichment history are reached. While Model 1 produces an excellent agreement with the N/C and N/O values derived from observations of H II regions and with the N/O values derived from metal poor stars, Model 1 is not able to produce a good fit for the N/O values derived from metal rich stars. Alternatively Model 2 produces a fair fit to the N/C and N/O values derived from metal rich stars, but fails to explain the H II region observations as well as those of metal poor stars. Consequently the N enrichment problem has to be studied further. A more precise discussion of the N enrichment history requires a solution of the observational discrepancy in the N/C and N/O values between the H II regions and the metal rich stars, as well as a revision of the N yields available.

Models 1 and 2 predict an enrichment in the O/H ratio of 0.13 dex since the Sun was formed. By adding this value to the Asplund et al. (2005) $12 + \log \text{O/H} = 8.66$ solar value, we predict for the ISM in the solar vicinity a value of $12 + \log \text{O/H} = 8.79$ in excellent agreement with the value derived from the recombination line observations, after correcting by the dust presence, that amounts to $12 + \log \text{O/H} = 8.77 \pm 0.05$.

Models 1 and 2 predict an increase in the C/H ratio of 0.29 dex and 0.26 dex since the Sun was formed. By adding these values to the Asplund et al. (2005) $12 + \log \text{C/H} = 8.39$ solar value, we predict for the ISM in the solar vicinity values of $12 + \log \text{C/H} = 8.68$ and 8.65 in excellent agreement with the value derived from the recombination line observations, after correcting by the dust presence, that amounts to $12 + \log \text{C/H} = 8.67 \pm 0.07$.

From the values presented in Table 5 and Figure 3, it is clear that Model 1 produces a better fit to the H II region restrictions, to the solar values, and to the C/O versus O/H enrichment history than Model 2.

In this paper we present a solution to the C enrichment history of the Galaxy based on the yields and observations available. The solution is based on the adoption of C yields that increase with metallicity due to stellar winds in MS and decrease with metallicity due to stellar winds in LIMS. These yields fit the behavior of the C/O ratio in the $6 < r(\text{kpc}) < 11$ range, the range for which we have C/H and O/H values from H II regions based on

recombination lines. The adopted yields also produce a reasonable fit to the C/O history of the solar vicinity.

We also find that about half of the C in the ISM of the solar vicinity at the present time has been produced by MS and half by LIMS. Also, at the present time, for a Galactocentric distance of 6 kpc about 53 % of the C has been produced by MS and 45 % by LIMS, while for 11 kpc the opposite is true, about 42 % of the C has been produced by MS and 56 % by LIMS.

It is clear that a more powerful treatment of convection, a better value of the $^{12}\text{C}(\alpha,\gamma)^{16}\text{O}$ rate, and a more realistic mass loss rate scheme will produce a better solution to the C enrichment problem. Moreover to produce a more stringent test for the C yields it is necessary to obtain observations of the C/O ratio for $r < 6$ kpc and $r > 11$ kpc and to include a model of the bulge formation and its effect on the C/O values for the inner regions of the Galaxy.

We would like to thank Chris Akerman for providing us the observational errors of the C, O and Fe stellar values, as well as John Bahcall for relevant correspondence. We would like to thank also Dick Henry, the referee of this paper, for some excellent suggestions. We also acknowledge John Scalo for suggesting us the use of another IMF. LC and MP received partial support from CONACyT (grant 36904-E) and DGAPA UNAM (grant IN114601), respectively. CE and JGR received partial support from the Spanish Ministerio de Ciencia y Tecnología (MCyT) under projects AYA2001-0436 and AYA2004-07466.

REFERENCES

- Akerman, C. J., Carigi, L., Nissen, P. E., Pettini, M., & Asplund, M. 2004, *A&A*, 414, 931
- Asplund, M., Grevesse, N., & Sauval, A. J. 2005, in: *Cosmic Abundances as Records of Stellar Evolution and Nucleosynthesis*, ed. F. N. Bash & T. G. Barnes, ASP Conference Series, in press, astro-ph/0410214
- Bahcall, J. N., Basu, S., Pinsonneault, M. & Serenelli, A. M. 2004, *ApJ*, in press (astro-ph/0407060)
- Bresolin, F., Garnett, D. R., & Kennicutt, R. C. 2004, *ApJ*, 615, 228
- Carigi, L. 2000, *Rev. Mexicana. Astron. Astrofís.*, 36, 171
- Carigi, L. 2003, *MNRAS*, 339, 825
- Chiappini, C., Matteucci, F., & Meynet, G. 2003a, *A&A*, 410, 257

- Chiappini, C., Romano, D., & Matteucci, F. 2003b, MNRAS, 339, 63
- Chieffi A., & Limongi M. 2002, ApJ 577, 281
- Deharveng, L., Peña, M., Caplan, J., & Costero, R. 2000, MNRAS, 311, 329
- El Eid, M. F., Meyer, B. S., & The, L. S 2004, ApJ, 611, 452
- Esteban, C., García-Rojas, J., Peimbert, M., Peimbert, A., Ruíz, M. T., Rodríguez, M., & Carigi, L. 2004a, ApJ, in press, (astro-ph/0408397), (Paper I)
- Esteban, C., Peimbert, M., García-Rojas, J., Ruiz, M. T., Peimbert, A., & Rodríguez, M. 2004, MNRAS, in press (astro-ph/0408249)
- Esteban, C., Peimbert, M., Torres-Peimbert, S., & Escalante, V. 1998 MNRAS, 295, 401
- García-Rojas, J., Esteban, C., Peimbert, M., Rodríguez, M., Ruiz, M. T., & Peimbert, A. 2004, ApJS, 153, 501
- Gavilán, M., Buell, J. F., & Mollá, M. 2005, A&A, in press, (astro-ph-0411746)
- González, G., Laws, C., Tyagi, S., & Reddy, B. E., 2001 AJ, 285, 403
- Grevesse, N., & Sauval, A. J. 1998, Space Sci. Rev., 85, 161
- Henry, R. B. C., Edmunds, M. G., & Köppen, J. 2000, ApJ, 541, 660
- Herwig, F. & Austin, S. M. 2004, ApJ, 613, L73
- Hou, J. L., Prantzos, N., & Boissier, S. 2000, A&A, 362, 921
- Israelian, G., Ecuivillon, A., Rebolo, R., García-López, R., Bonifacio, P., & Molaro, P. 2004, A&A, 421, 649
- Kroupa, P., Tout, C.A., & Gilmore, G. 1993, MNRAS, 262, 545 (KTG)
- Liang, Y. C., Zhao, G, & Shi, J. R. 2001, A&A, 374, 936
- Maeder, A. 1992, A&A, 264, 105
- Marigo, P., Bressan, A., & Chiosi, C. 1996, A&A, 313, 545
- 1998, A&A., 331, 580
- Mathis, J. S., & Rosa, M. R. 1991, A&A, 245, 625

- Meynet G., & Maeder A. 2002, *A&A*, 390, 561
- Peimbert, M. 1967, *ApJ*, 150, 825
- Peimbert M., & Costero R., 1969, *Bol. Obs. Tonantzintla y Tacubaya*, 5, 3
- Pilyugin, L. S., Ferrini, F., & Shkvarun, R. V. 2003, *A&A*, 401, 557
- Portinari, L., Chiosi, C., & Bressan, A. 1998, *A&A*, 334, 505 (PCB98)
- Prantzos, N. 2003, *Rev. Mexicana. Astron. Astrofís. S.C.* 17, 121
- Sadakane, K., Ohkubo, M., Takeda, Y., et al. 2002, *PASJ*, 54, 911
- Salpeter, E.E. 1955, *ApJ*, 121, 161
- Santos, N. C., Israelian, G., & Mayor, M. 2000 *A & A*, 363, 228
- Scalo, J.M. 1986, *Fund. Cosmic. Phys.*, 11, 1
- Shaver, P. A., McGee, R. X., Newton, L. M., Danks, A. C., & Pottasch, S. R. 1983, *MNRAS*, 204, 53
- Takeda, Y., Sato, B., Kambe, E., et al. 2001, *PASJ*, 53, 1211
- Thielemann, F.K., Nomoto, K., & Hashimoto, M. 1993, in “Origin and Evolution of the Elements” eds. N. Prantzos et al., Cambridge University Press, p. 297
- van der Hoek, L. B., & Groenewegen, M. A. T. 1997, *A&AS*, 123, 305
- Woosley, S. E., & Weaver, T. A. 1995, *ApJS*, 101, 181 (WW95)

Table 1. N abundances in Galactic H II regions ^a

H II region	r (kpc)	t^2	$12 + \log(\text{N}/\text{H})$
M 16	6.34	0.036 ± 0.006	8.07 ± 0.12
M 8	6.41	0.037 ± 0.004	7.94 ± 0.06
M 17	6.75	0.033 ± 0.005	7.87 ± 0.13
M 20	7.19	0.036 ± 0.013	7.89 ± 0.09
NGC 3576	7.46	0.038 ± 0.009	7.87 ± 0.09
Orion neb.	8.40	0.022 ± 0.002	7.73 ± 0.15
NGC 3603	8.65	0.040 ± 0.008	7.89 ± 0.15
S 311	10.43	0.038 ± 0.007	7.61 ± 0.07

^aGaseous abundances. Galactocentric distances from Paper I.

Table 2. Present-day radial gradients

Model	Assumed Yields			C/O	
	MS $0 < Z < 0.02$	MS $Z \geq 0.02$	LIMS	value (dex) $r = r_{\odot} = 8 \text{ kpc}$	slope (dex kpc ⁻¹) $6 < r/\text{kpc} < 11$
1	MM02	M92	MBCP	−0.122	−0.057
2	MM02	M92	vdHG.var	−0.172	−0.053
3	MM02	M92	vdHG.const	−0.249	−0.066
4	MM02	M92	MM02	−0.350	−0.068
5	MM02	MM02	MBCP	−0.279	−0.025
6	MM02	MM02	vdHG.var	−0.355	−0.012
7	MM02	MM02	vdHG.const	−0.410	−0.029
8	MM02	MM02	MM02	−0.542	−0.024
9	PCB98	PCB98	MBCP	−0.142	−0.004
10	WW95	WW95	vdHG.var	−0.163	−0.014
11	WW95	WW95	vdHG.const	−0.463	−0.005
Obs ^a				-0.102 ± 0.080	-0.058 ± 0.020

^aPaper I values corrected by dust, see section 2

Table 3. Carbon budget for the solar vicinity ^a

Model	Contribution (per cent)		
	MS	LIMS	SNIa
1	48.2	49.8	2.0
2	50.2	47.2	2.6
3	59.5	38.0	2.5
4	75.3	21.8	2.9
5	40.2	57.5	2.3
6	40.8	56.4	2.8
7	52.7	44.4	2.9
8	70.0	26.1	3.9
9	51.8	47.0	1.2
10	36.2	62.3	1.5
11	66.7	32.1	1.9

^aPercentage of C in the ISM produced by different types of stars over a period of 13 Gyr.

Table 4. Carbon budget for different Galactocentric distances ^a

r (kpc)	Contribution (per cent)		
	MS	LIMS	SNIa
	Model 1		
4	57.0	40.8	2.2
6	53.4	44.6	2.0
8	48.2	49.8	2.0
11	42.4	55.5	2.1
16	40.8	57.2	2.1
	Model 2		
4	63.1	34.0	2.9
6	58.0	39.3	2.7
8	50.2	47.2	2.6
11	38.6	59.0	2.4
16	30.3	67.6	2.1

^aPercentage of C in the ISM produced by different types of stars over a period of 13 Gyr.

Table 5. ISM abundance values ^a

	O/H	C/H	N/H	Fe/H	C/O
At the time the Sun was formed ($t = 8.43$ Gyr)					
Model 1	8.66	8.38	7.56	7.46	-0.28
Model 2	8.66	8.36	7.89	7.49	-0.30
Solar ^b	8.66 ± 0.05	8.39 ± 0.05	7.78 ± 0.05	7.45 ± 0.05	-0.27 ± 0.07
At the present time ($t = 13.0$ Gyr)					
Model 1	8.79	8.67	7.84	7.72	-0.12
Model 2	8.79	8.62	8.13	7.75	-0.17
H II Regions	8.77 ± 0.05 ^c	8.67 ± 0.07 ^c	7.84 ± 0.10 ^d	--	-0.10 ± 0.08 ^c

^aGiven in $12 + \log (X/H)$.

^bAsplund et al. (2005).

^cPaper I values corrected by dust.

^dThis paper.

Table 6. Nitrogen budget for different Galactocentric distances ^a

r (kpc)	Contribution (per cent)		
	MS	LIMS	SNIa
	Model 1		
4	44.5	53.5	2.0
6	40.2	58.0	1.8
8	33.5	64.7	1.8
11	23.6	74.5	1.8
16	12.0	86.0	2.9
	Model 2		
4	26.6	68.8	4.7
6	23.7	72.0	4.3
8	19.2	76.7	4.1
11	12.7	83.6	3.7
16	6.3	90.1	3.2

^aPercentage of N in the ISM produced by different types of stars over a period of 13 Gyr.

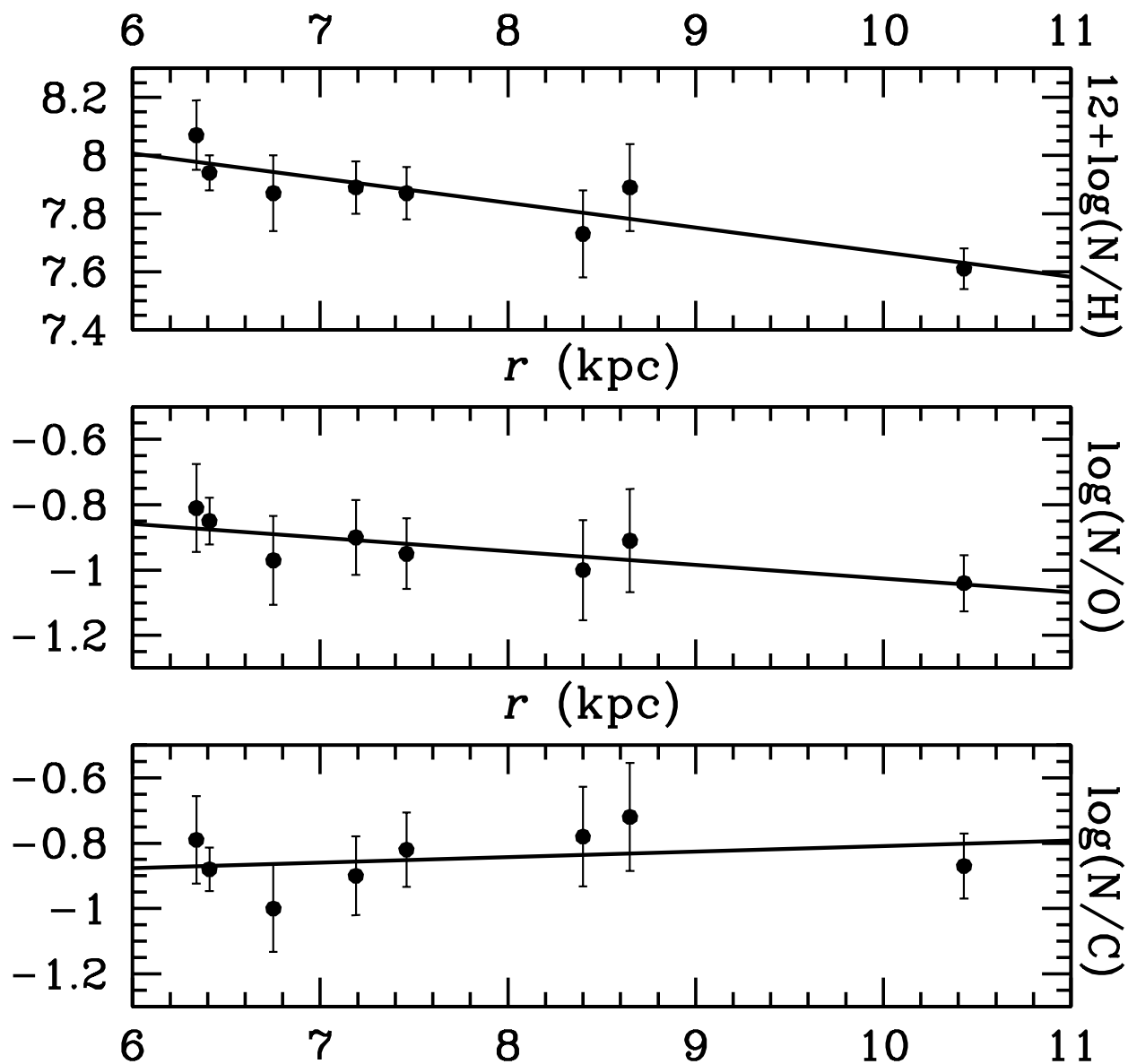


Fig. 1.— N/H , N/C , and N/O radial abundance gradients of the Galactic disk derived from H II regions. The N abundances have been determined from collisionally excited lines while those of H , C and O have been obtained from recombination lines (see Table 1 and Paper I). The lines indicate the least-squares linear fits to the data.

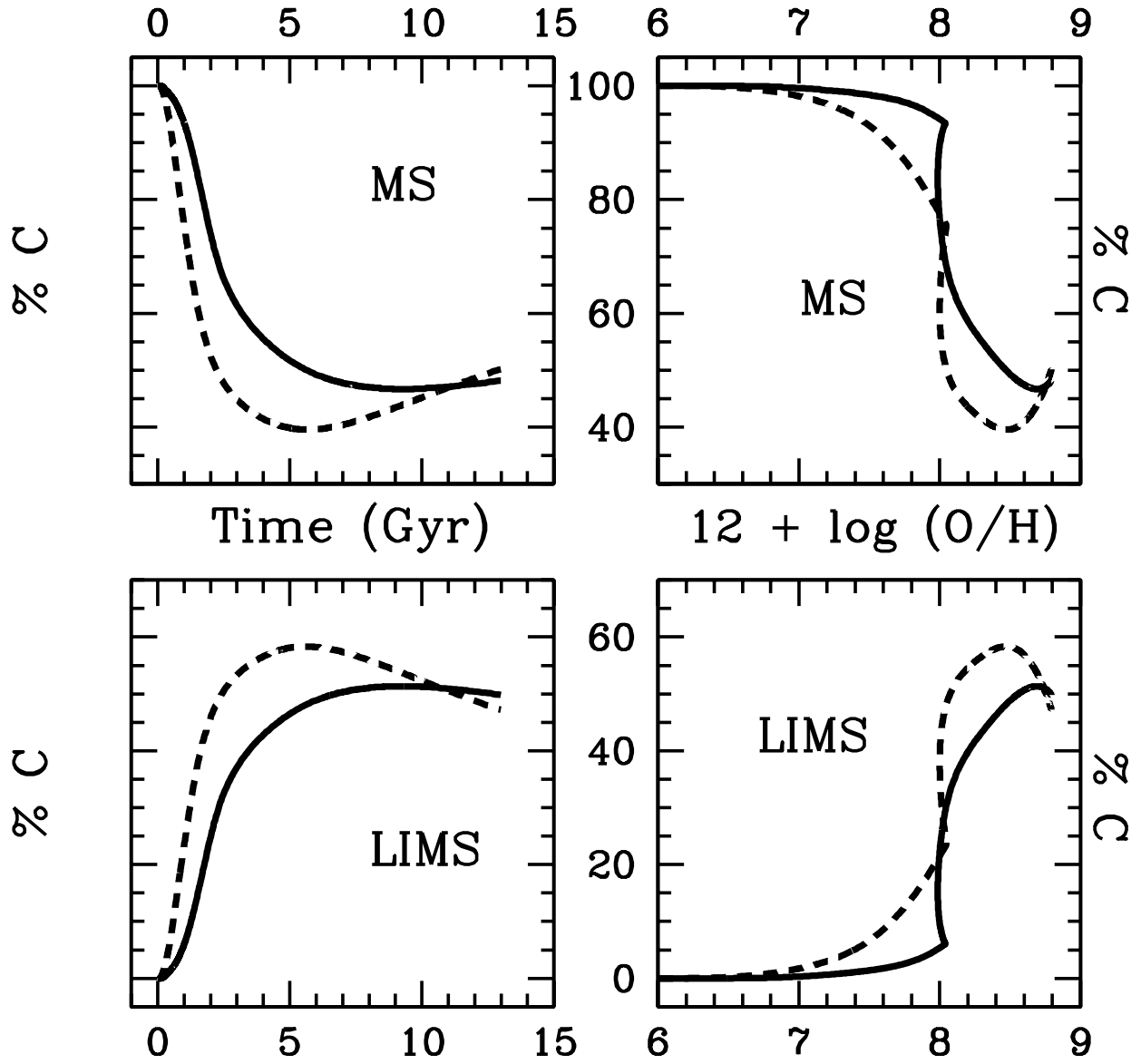


Fig. 2.— Cumulative percentage of C as a function of time and $12 + \log(O/H)$, due to massive stars (MS), and low and intermediate-mass stars (LIMS) at the solar vicinity. Solid lines represent Model 1 and broken lines represent Model 2.

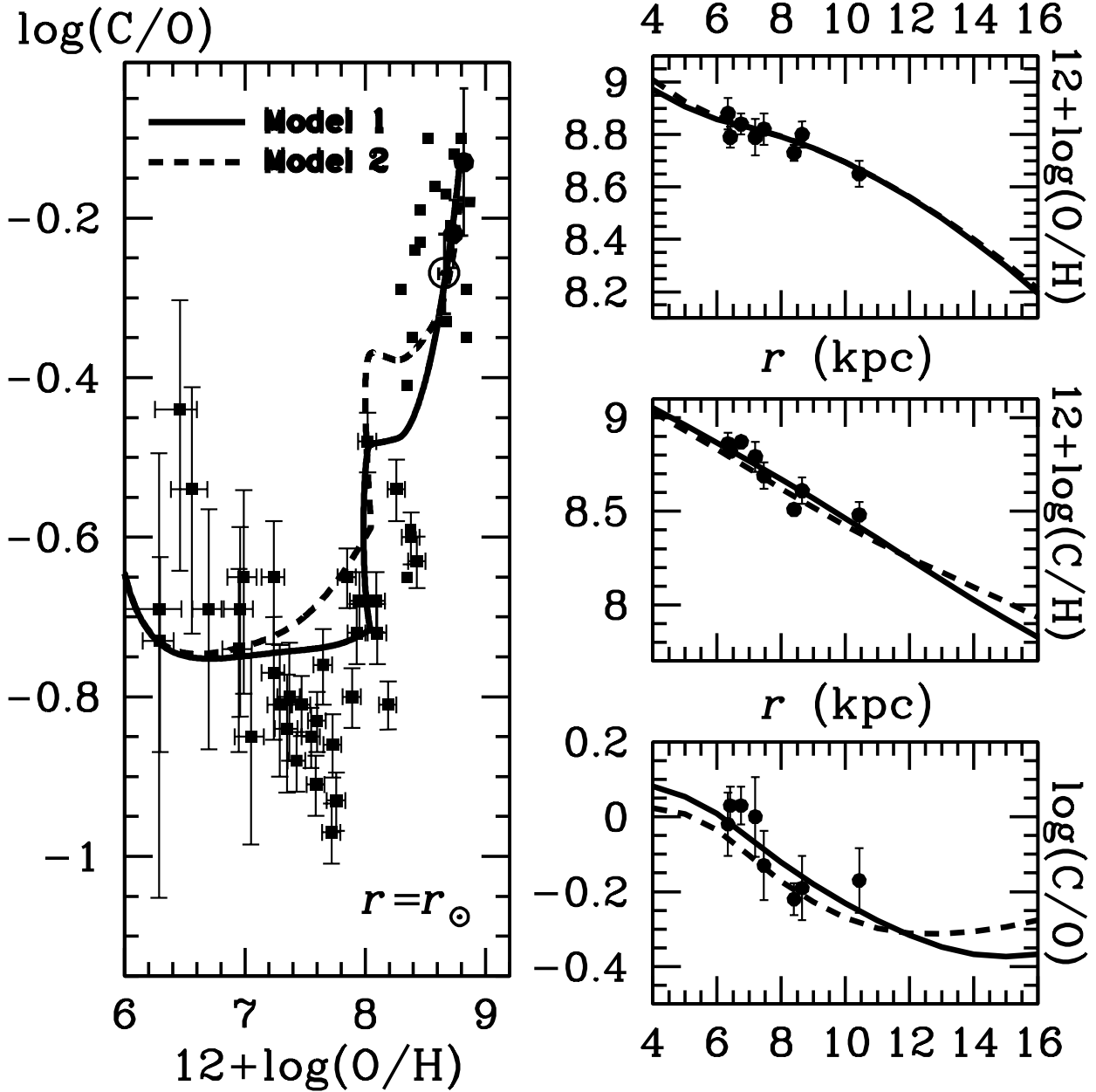


Fig. 3.— Predictions from models considering: a) for massive stars, yields by Chieffi & Limongi (2002) for $Z = 0.0$, yields by Meynet & Maeder (2002) for $10^{-5} < Z < 0.004$, Maeder (1992) for $Z = 0.02$; and, b) for low and intermediate mass stars, yields by Marigo et al. (1996, 1998) and Portinari et al. (1998) (Model 1), or van den Hoek & Groenewegen (1997) with η variable (Model 2). The left panel shows the C/O evolution in the ISM of the solar vicinity with O/H. The right panels show the present-day ISM abundance ratios as a function of Galactocentric distance. *Filled circles*: H II regions, gas plus dust values; the gaseous values from Paper I have been corrected by the dust fraction (see section 2). *Filled squares*: dwarf stars from Akerman et al. (2004). \odot : Solar values from Asplund et al. (2005).

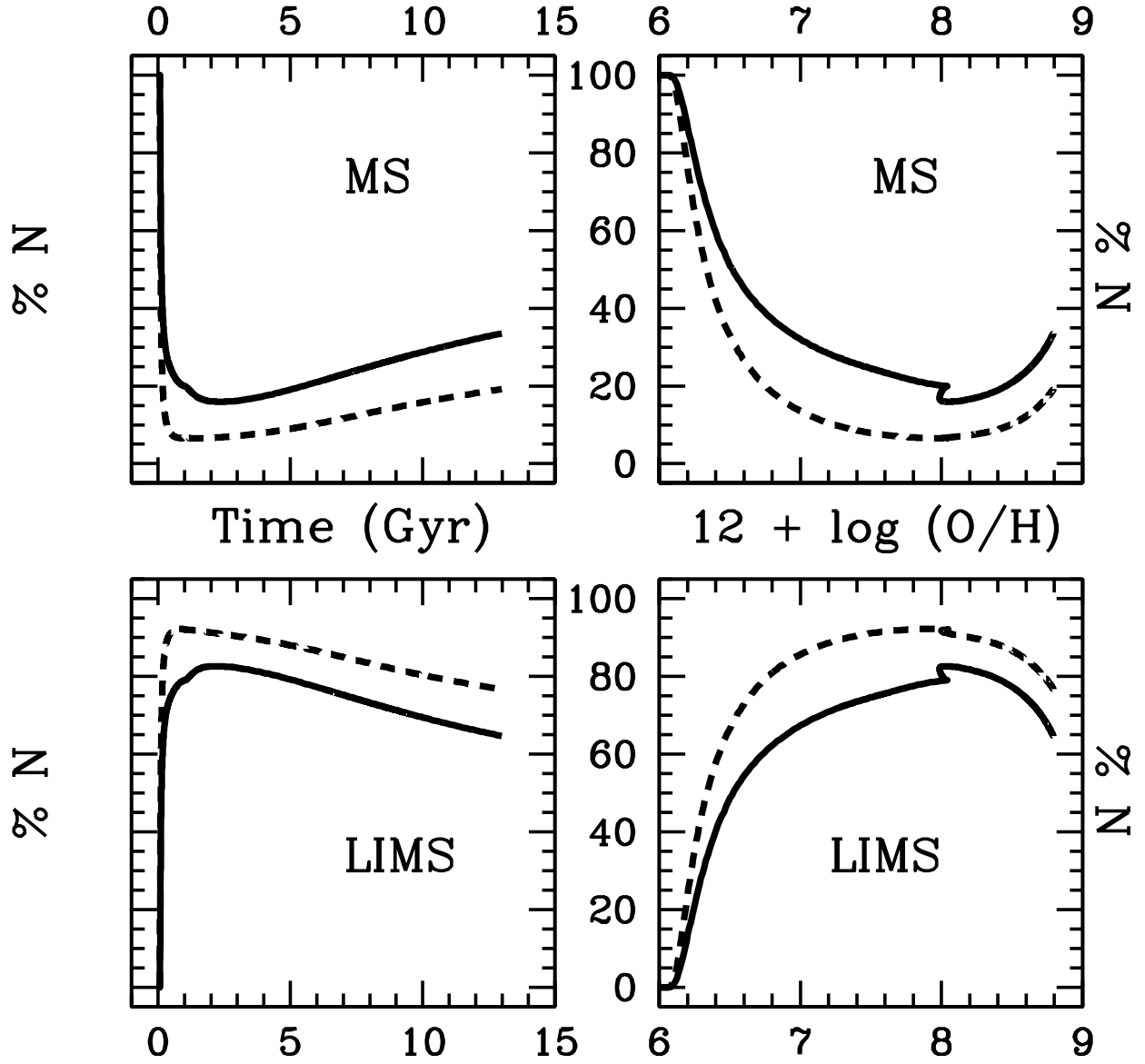


Fig. 4.— Cumulative percentage of N as a function of time and $12 + \log(O/H)$, due to massive stars (MS), and low and intermediate-mass stars (LIMS) at the solar vicinity. Solid lines represent Model 1 and broken lines represent Model 2.

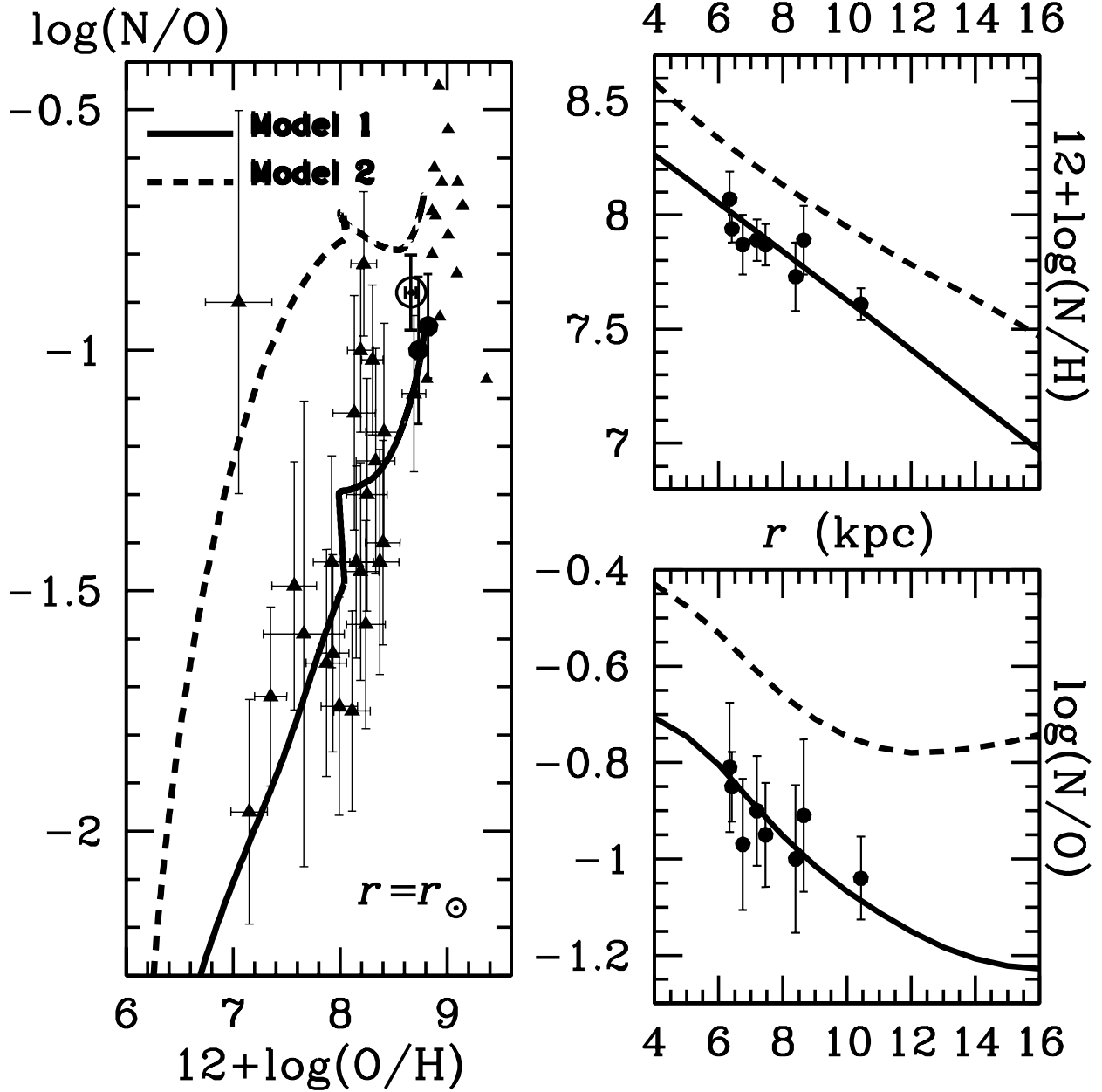


Fig. 5.— N/H and N/O gradients in the Galactic disk and N/O versus O/H enrichment history in the solar vicinity. The left panel shows the N/O evolution in the ISM of the solar vicinity with O/H. The adopted N yields for $Z = 0.02$ are those by Meynet & Maeder (2002), all the other yields are as in Fig. 3 (see section 3). The right panels show the present-day ISM abundance ratios as a function of Galactocentric distance. *Filled circles*: H II region values presented in Fig. 1, *Filled triangles*: unevolved main sequence stars from Israelian et al. (2004), \odot : solar values from Asplund et al. (2005).

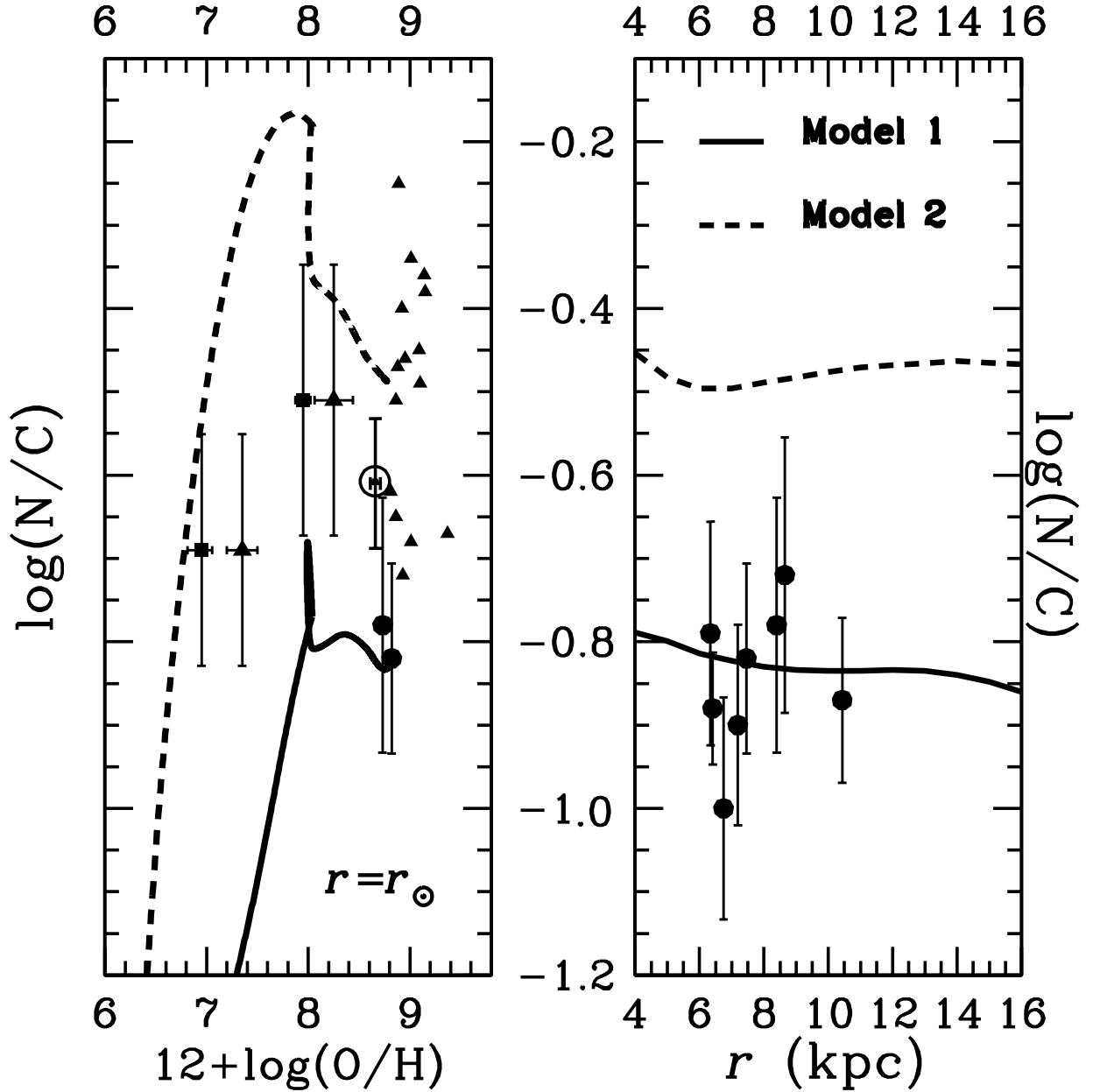


Fig. 6.— N/C gradients in the Galactic disk and the N/C versus O/H enrichment history in the solar vicinity. The left panel shows the N/C evolution in the ISM of the solar vicinity with O/H. The right panel shows the present-day ISM abundance ratios as a function of Galactocentric distance. *Filled circles*: H II region values presented in Fig. 1, *filled triangles*: unevolved stars from Santos et al. (2000), Takeda et al. (2001), González et al. (2001), Sadakane et al. (2002), and Israelian et al. (2004). \odot : solar values from Asplund et al. (2005).

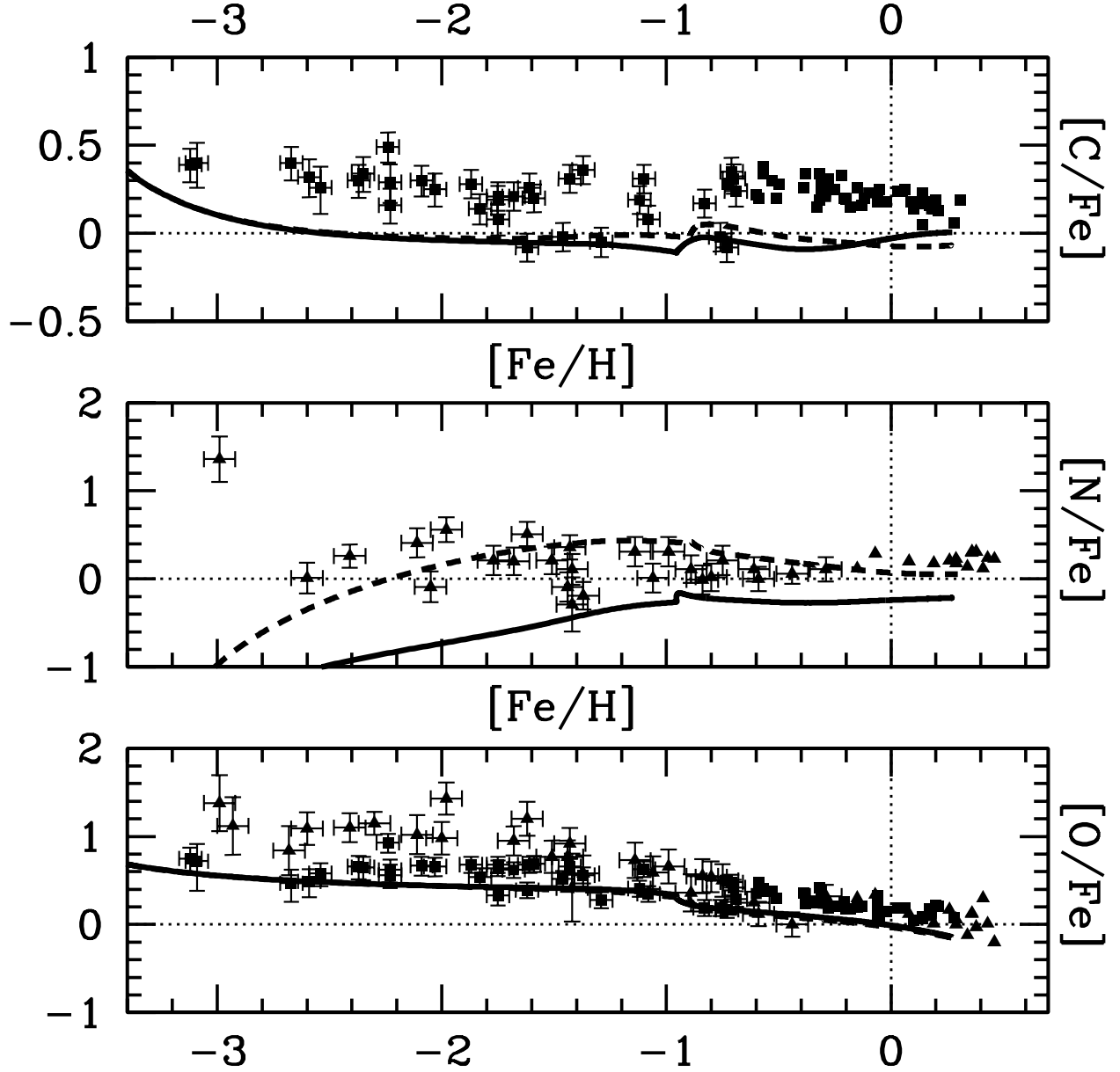


Fig. 7.— $[C/Fe]$, $[N/Fe]$, and $[O/Fe]$ vs $[Fe/H]$ in the solar vicinity. *Filled triangles*: Un-evolved stars from Israelian et al. (2004), *filled squares*: dwarf stars from Akerman et al. (2004). Solid lines represent Model 1 and broken lines represent Model 2.